SECOND EUROPEAN CONFERENCE ON EARTHQUAKE ENGINEERING
AND SEISMOLOGY, ISTANBUL AUG. 25-29, 2014

ESTIMATION OF THE GROUND MOTION IN THE EPICENTRAL REGION OF THE ATHENS, GREECE (1999) EARTHQUAKE

Evangelos AVGENAKIS[1], Ioannis PSYCHARIS[2] and Ioannis TAFLAMPAS[3]

ABSTRACT

On September 7th, 1999 an earthquake of magnitude M_w = 5.9 rocked the city of Athens. It is considered one of the most significant natural disasters in the modern history of Greece. In this paper, recent developments on the characteristics of near-fault ground motions are used in order to estimate the shaking at the epicentral region taking under consideration directivity phenomena. Using the available records, most of which contain well correlated velocity pulses with a similar period at all sites, compatible with the expected value for the moment magnitude of the earthquake, it is shown that the corresponding sites were affected by forward directivity phenomena. As no strong motion records exist for the most damaged areas, this information was used to estimate the ground motion at the epicentral region through reverse analysis procedures. To this end, the nonlinear response of a four-storey reinforced concrete building in Thrakomakedones, one of the most affected areas, was computed under several scenarios of base excitation and the expected damage was compared with the recorded one. The ground motions examined for this location were derived by matching several recorded ground motions with the elastic spectra proposed by Boore and Atkinson (2008), properly modified to account for directivity effects according to Shahi and Baker (2011). Based on these results, mean response spectra are proposed for the examined location. It is noted that the estimated *PGA* of the ground motion is larger than what it was believed up to now.

INTRODUCTION

The main shock of the Athens September 7th, 1999 earthquake occurred at a distance of about 18 km from the historical center of the city. Almost 100 buildings collapsed causing 143 deaths, 800 structures were seriously damaged and 65000 suffered smaller damage. The first days after the earthquake 100000 people remained homeless and the economic loss was estimated to about 3 billion US$. From that point of view, the Athens earthquake was the most significant natural disaster in the modern history of Greece.

The event was caused by a normal fault dipping to the south (Fig. 1). The fault plane was characterized of a dipping angle of 52° and a strike angle of 117°. The rupture had a focal depth of 12 km and propagated with a number of sub-events towards the eastern region of the fault and the city center. The mostly damaged area was associated with the eastern regions of the rupture zone, an indication of possible near fault directivity effects. Unfortunately, however, there were no recordings of the ground motion in that area (Fig. 1).

[1] Graduate student, National Technical University, Athens, Greece, vavgen@outlook.com
[2] Professor, National Technical University, Athens, Greece, ipsych@central.ntua.gr
[3] Civil Engineer, Ph.D., National Technical University, Athens, Greece, taflan@central.ntua.gr

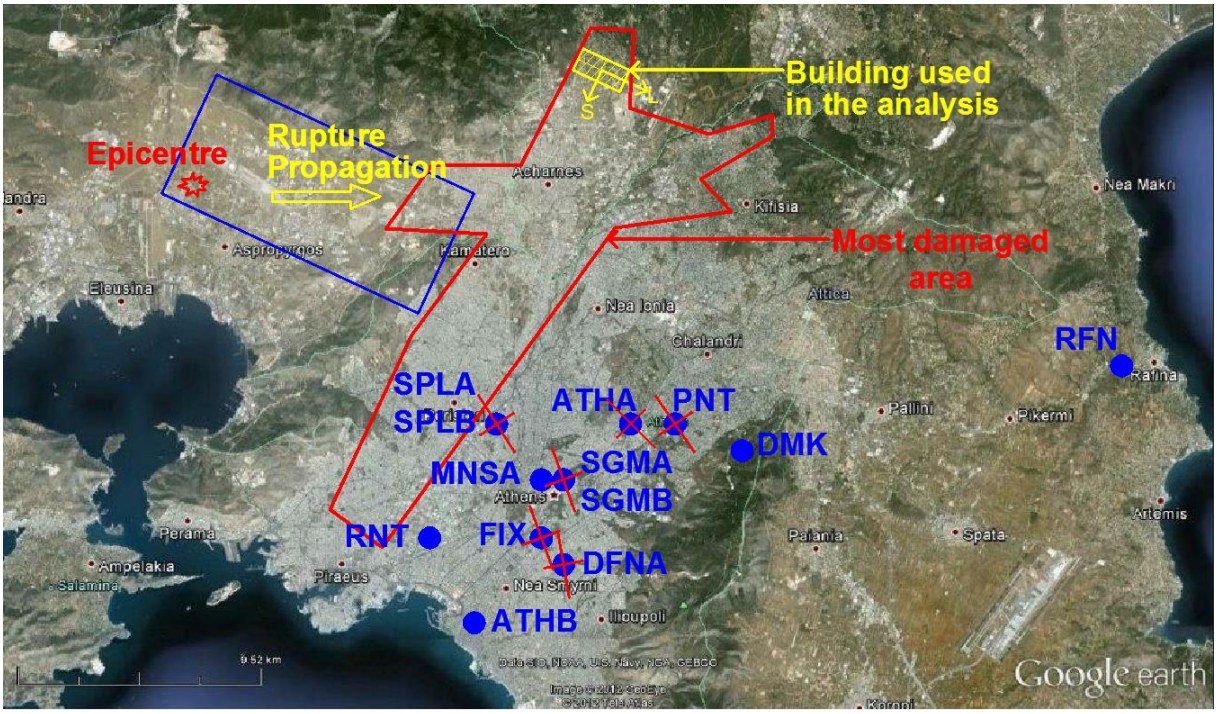

Figure 1. Map of the fault and the most damaged area, recorded ground motions, directivity pulse directions and examined building location (modified from Elenas 2003)

During the last decades, serious effort has been devoted to estimate the expected ground motion and associated spectral values in the near field region (Bertero *et al.* 1978, Abrahamson and Silva 1997, Somerville *et al.* 1997, Somerville 1998 and 2003). This research showed that the ground motion close to the causative fault can be substantially different from typical records obtained at large distances, especially if it is affected by forward directivity effects. The main feature of forward directivity is the existence of velocity pulses in the ground motion, caused by the spreading of the fault rupture towards the examined site. Directivity phenomena depend on the azimuth of the site and its distance from the fault plane and are especially prominent in the normal-to-the-rupture component (fault-normal component).

The most important feature of pulse-like ground motions is a bell-shaped enlargement of the spectral accelerations in a range of periods around the characteristic period of the directivity pulse (Shahi and Baker 2011). This increase in spectral accelerations in the medium to long period range has also a prominent effect on the inelastic response spectra, since the ductility demand is amplified for periods less than one half of the characteristic pulse period and, furthermore, the relevant deformation increases abruptly (Iervolino and Cornell 2008).

In this paper, recently proposed techniques for the identification of near field pulses (Shahi and Baker 2011, Rowshandel 2006) are applied to the available records of the Athens earthquake in order (a) to investigate the possible correlation of the mostly damaged area with near field directivity phenomena and (b) to estimate the ground motion in the epicentral region. For the former, several parameters were utilized, as the ratio of the pulse-like over the non-pulse-like component of each record, the period of the directivity pulse, etc. For the latter, the nonlinear response of a four-storey reinforced concrete building in Thrakomakedones was computed under several scenarios of base excitation, derived by matching the recorded ground motions with the elastic spectra proposed by Boore and Atkinson (2008) properly modified to account for directivity effects according to Shahi and Baker (2011), and the expected damage was compared with the recorded one. Based on these results, mean response spectra are proposed for the examined location.

ESTIMATION OF POSSIBLE GROUND MOTIONS

The most affected area during the Athens earthquake was located in a north-south direction along the eastern edge of the causative fault (Fig. 1). Considering that the fault ruptures in a west-east direction across the fault surface, it appears that the affected area spreads along a direction normal to the rupture permitting the assumption of directivity effects. This assumption is further founded by the model proposed by Rowshandel (2006) according to which, if the vector from the epicenter to the rupture asperities presents a direction close to that of the vector from the asperities to the examined site, as it happened during the Athens event, then the site is affected by directivity phenomena. This model appears to be more effective than the one presented by both Somerville (1997) and Shahi and Baker (2011) in which, for dip slip faults, the dip vector of the fault coincides with the rupture vector and the directivity effects are expected across the fault trace. This model presents only a 30% correlation with existing cases.

The Athens earthquake was recorded at several places, in the center and the suburbs of the city (Fig. 1 and Table 1), but not in the most damaged areas. The available records were rotated in order to find the direction of the strongest component. The appropriate rotation for each record was chosen so that the largest amplitude associated with the ground velocity pulse was attained. The largest component of the rotated records are oriented between 140 and 160 degrees with respect to the north (clockwise). The results are depicted in Fig. 1, in which the amplitude of the ground motion in the direction of the strongest component and in the normal to it are shown. It is seen that, in most case, the strongest component has approximately N-S direction, normal to the direction of the rupture propagation. In the same figure, the location and direction of the building examined later in this paper is indicated.

Table 1. Recording sites and their characteristics of the Athens 1999 earthquake (Psycharis *et al*. 1999)

No.	Code	Site	Geology	Place	Epic. dist. [km]	max Acceleration [g]		
						L	V	T
1	MNSA1	Monastiraki	Schist of bad quality, black soft phylite, archaeological deposits, underground caves	Free field	17	0.223	0.223	0.534
2	ATHA1	Neo Psychiko	Tertiary deposits	Basement, 3-story bldg	18	0.083	0.121	0.104
3	DMK1	Ag. Paraskevi	Limestone	Free field	19	0.052	0.042	0.073
4	FIX1	Sygrou-FIX	Limestone / Sandstone of good quality	Metro station, level –1	19	0.086	0.046	0.122
5	SGMA1	Syntagma	Limestone / schist	Metro station, level –1	18	0.146	0.051	0.239
6	SGMB1	Syntagma	Limestone / schist	Metro station, level –3	18	0.115	0.088	0.092
7	SPLA1	Sepolia	Deposits of Kifissos river	Metro station, level –1	15	0.248	0.093	0.226
8	SPLB1	Sepolia	Deposits of Kifissos river	Basement, 2-story steel bldg	15	0.356	0.204	0.326
9	DFN1	Dafni	Schist	Metro station, level –2	21	0.038	0.041	0.112
10	PNT1	Papagos	Tertiary deposits	Metro station, level –2	19	0.090	0.057	0.080
11	ATH02	Chalandri	Alluvial deposits	Basement, 2-story bldg	17	0.130	0.190	0.110
12	ATH03	Pireos str – KEDE	Alluvial deposits	Ground floor, 1-story bldg	16	0.290	0.350	0.190
13	ATH04	Kypseli	Schist	Basement, 4-story bldg	16	0.140	0.120	0.060
14	KERA	Keratsini	Soft rock	Basement, Administr. bldg	15	0.186	0.220	0.157

The velocity time histories and the acceleration and velocity response spectra of the rotated ground motions present distinctive pulses of periods ranging from about 1.4 sec for records on stiff soil (e.g. records SGMA and SGMB at the historical center of the city) to 2.1 sec for records on soft soil deposits (e.g. SPLA and SPLB records). These values correlate well with regression formulas available in the literature. For example, Cioccarelli and Iervolino (2010) used the NGA database and proposed the following relationship between the mean pulse period, T_p, and the moment magnitude of the earthquake, M_w:

$$lnT_p = -6.19 + 1.07M_w \quad (1)$$

The standard deviation was calculated to 0.59. Applying this formula to Athens earthquake of magnitude M_w = 5.9 leads to T_p = 1.13 sec for the mean value and to T_p = 2.04 sec for the mean value plus one standard deviation. This period range is close to the observed pulse periods.

A further indicator for the existence of directivity pulses in a record's velocity time history is the shape of the ratio between the acceleration response spectra of the original record and the produced residual, after the subtraction of what is considered as a directivity velocity pulse (Shahi and Baker 2011). This ratio is a measure of the spectral amplification in the medium- to long-period range between pulse-like and non-pulse-like records, indicated by Somerville et al (1997). According to Shahi and Baker, the amplification, A_f, which is the ratio between the original ground motion containing the directivity pulse and the residual ground motion after the removal of the pulse, presents a bell-shaped form around the pulse period, T_p, which can be expressed by the following mean function:

$$\mu_{lnAf} = \begin{cases} 1.131 \exp\left(-3.11\left(\ln\left(T/T_p\right) + 0.127\right)^2\right) + 0.058, & T \leq 0.88T_p \\ 0.896 \exp\left(-2.11\left(\ln\left(T/T_p\right) + 0.127\right)^2\right) + 0.255, & T > 0.88T_p \end{cases} \quad (2)$$

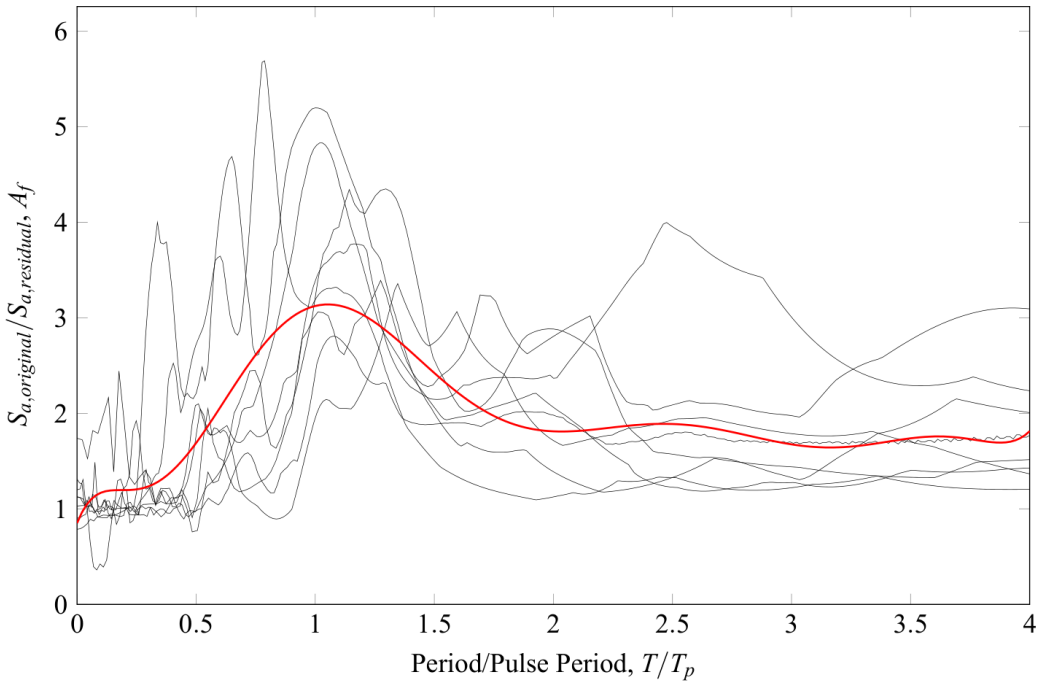

Figure 2. Ratio of original to residual elastic spectra of recorded ground motions in respect to the ratio of the period to the pulse period and "mean" spectral amplification due to directivity pulses

This ratio was calculated for the records obtained during the Athens earthquake and the results are shown in Fig. 2. The mean curve (red line) definitely has a bell shaped form and correlates well with the mean function proposed by Shahi & Baker. For example, the amplification for $T = T_p$ is about 3, while the corresponding value of A_f according to Eq. (2) is 3.1.

Furthermore, the residual ground motion spectra were compared with the spectra proposed by Boore and Atkinson (2008) for non pulse-like records derived by empirical regression of the extensive PEER NGA database. Equations are provided for the peak ground acceleration, *PGA*, the peak ground velocity, *PGV*, and the pseudo-spectral acceleration values at periods between 0.01 sec and 10 sec. The main variables of the Boore-Atkinson relationships are the moment magnitude, M_w, the closest horizontal distance to the surface projection of the fault plane (Joyner-Boore distance), R_{JB}, and the time averaged shear-wave velocity from the surface to a depth of 30 m, V_{s30}. The form of the equations is:

$$\ln Y = F_M(M_w) + F_D\left(R_{JB}, M_w\right) + F_S\left(V_{s30}, R_{JB}, M_w\right) + \varepsilon \cdot \sigma_T \tag{3}$$

where, F_M, F_D and F_S represent magnitude scaling, distance function and site amplification respectively, σ_T is the standard deviation of a single predicted value of $\ln Y$ away from its mean value and ε is the fractional number of standard deviations. The fault type is an optional prediction variable that enters into the magnitude scaling term. The variable Y represents the peak ground acceleration, the peak ground velocity or the spectral values. The site amplification is given a linear and a nonlinear term. The nonlinear term depends on the variable PGA_{nl} which is the predicted *PGA* for V_{s30} = 760 cm/sec.

For the available records of the Athens earthquake, it was found that the residual ground motion spectra have values that are inside the confidence limits of the Boore & Atkinson spectra. Therefore, it appears that the residual (high-frequency component) of the ground motion at any site can be approximated by these spectra. Adding the amplification proposed by Shahi & Baker in order to take into account the effect of the directivity pulse, the response spectrum at any site can be estimated.

In order to compute the time-history of the ground motion in the epicentral region more accurately, a reverse analysis procedure was applied, utilizing the above-mentioned information on the directivity pulse of the event. To this end, the nonlinear response of a four-storey reinforced concrete building in Thrakomakedones, one of the most affected areas, was calculated for several scenarios of the base excitation and the computed damage was compared with the recorded one. The ground motions considered in these analyses were derived by matching the recorded ground motions with the expected elastic spectra according to the above-mentioned procedure, i.e. by modifying the Boore & Atkinson spectra to account for directivity effects according to Shahi and Baker (2011).

Specifically, the following procedure was followed: First, the Boore & Atkinson spectra were calculated for normal fault using the following values: M_w = 5.9, R_{jB} = 7 km, V_{s30} = 780 m/sec, which reflect the seismic event and the examined location. Various values for the fraction ε of the standard deviation were considered in order to develop several ground motion scenarios, the validity of which was checked on the basis of the produced damage to the examined building, as will be explained in the ensuing. The calculated spectra were modified according to Shahi & Baker, using an estimated value for the period of the pulse T_p = 1.6 sec, which is thought to correspond to the specific soil conditions. Indicative spectra produced in this way are presented in Fig. 3 for various standard deviations. Spectra with directivity effects are denoted with D (dashed lines) and ones without directivity effects with N (solid lines).

The accelerograms used in the non-linear time-history analyses of the building were produced according to the following procedure: First, six of the recorded accelerograms were chosen (ATHA, DFNA, DMK, FIX, SGMA, SGMB), specifically those recorded on stiff soils or rock, since the building is founded on firm ground. The selected records were rotated in the main directions of the building. The rotated accelerograms were matched to the developed spectra, with or without considering the directivity pulse, according to the above-mentioned methodology, using the program SeismoMatch (Seismosoft), for various peak ground accelerations. In Fig. 4, examples of the produced accelerograms, based on the original records mentioned above and corresponding to standard deviation ε = 3.1 are presented. In this case, directivity effects were included only in the longitudinal direction of the building (see Fig. 1). It is noted that the matching procedure cannot fully match elastic spectra in very low periods, therefore, the peak ground accelerations of the produced accelerograms do not coincide with the *PGA*s that correspond to the target spectra. However, in the period range of interest, target spectra are matched sufficiently well.

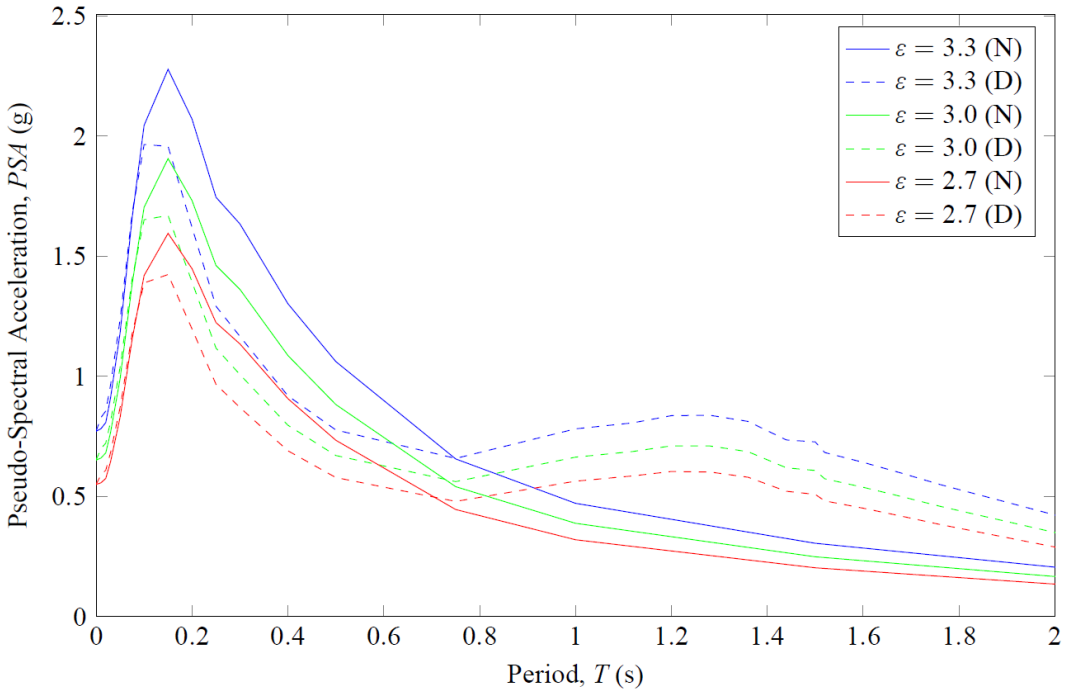

Figure 3. Example of produced elastic spectra for the specific site for various standard deviations. (D) means that directivity effects have been considered, (N) that they have not.

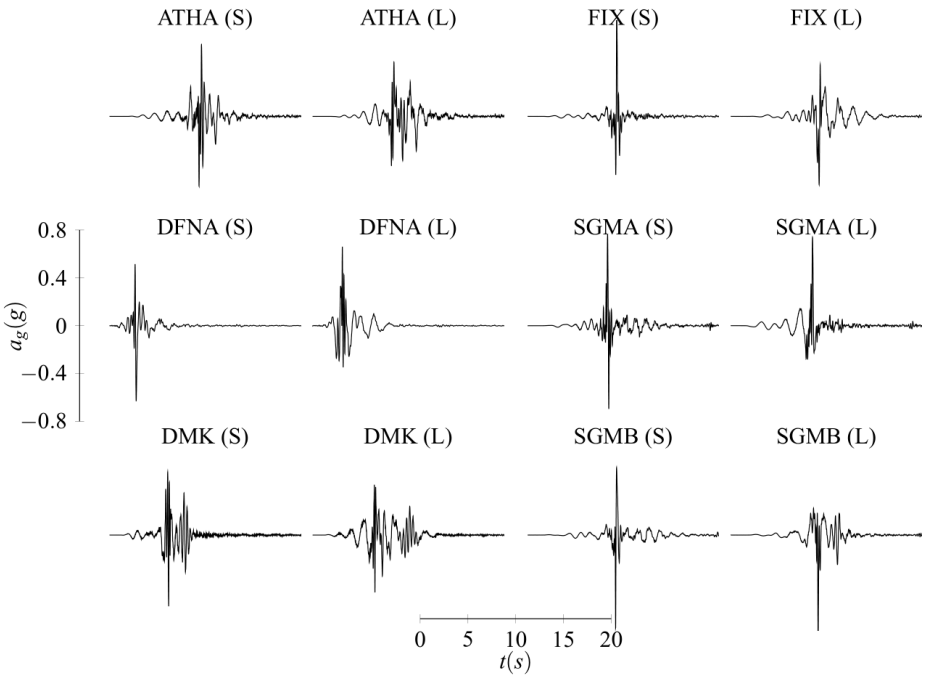

Figure 4. Example of produced accelerograms, corresponding to spectra with standard deviation ε = 3.1 in the short (S) and the long (L) direction of the building under consideration. Directivity effects were considered only in the long direction. The notation of the records refers to the original records used in each case.

MODELLING AND ANALYSIS OF THE EXAMINED BUILDING

The building examined is located in Thrakomakedones (Fig. 1), an area that was heavily damaged during the Athens '99 earthquake. It has an approximately rectangular plan with dimensions 21 m × 12 m with the longitudinal sides oriented to N65W direction. The building has four floors: an

underground floor with reinforced concrete perimeter walls; the ground floor without infill walls; and two residential floors with brick infill walls. The load bearing frame consists of reinforced concrete members. It is founded on rock, so fixed supports were used for the underground floor.

It is noted that the structure was designed with the old Greek seismic code (put in force in 1959, improved in 1985 and replaced by a modern code in 1995) without any specific seismic resistance details, which are specified in modern seismic codes to guarantee adequate ductile behaviour, such as closely spaced hoops in critical regions, extension of hoops inside the joints, etc. Due to that, many shear failures occurred during the earthquake, especially to columns and shear walls of the ground floor. Most of these failures were found to have direction parallel to the long direction of the building, which might be related to possible directivity phenomena, since this direction is close to the strong component of the ground moton (Fig. 1).

In order to estimate the actual ground motion at the site of the building, the expected damage under the derived synthetic accelerograms was compared with the recorded one. To this end, the model of the building was constructed so that all the details that could affect the response would be considered as accurately as possible. Thus, the beams were divided in three parts and the effective width of each part was calculated according to EC8 (for the end parts) and EC2 (for the middle one); rigid parts were considered at beam-column joints; the diaphragm effect of the slabs was modelled using stiff diagonal members; the basement perimeter walls were also modelled using diagonal members; the stiffness and the resistance of the infill walls was included in the numerical model with nonlinear strut elements. The materials were considered with their mean strength without any safety factor and P-Delta effects were taken into account for column members.

For the modelling details of the building, especially in what concerns the inelastic behaviour of the potential plastic hinges, the Greek Retrofitting Code (2012) (acting as an extension to EC8-3) was applied. According to this modelling approach, the concentrated plasticity model was used with zero length elements at member ends and properly modified member stiffnesses, as proposed by Ibarra and Krawinkler (2005). This model is able to account for observed RC member nonlinearities apart from flexural deformations, such as shear cracking, shear deformation and anchorage slip, phenomena that seem to strongly influence the response of reinforced concrete member during seismic excitation.

Special care was paid to the correct modelling of shear failure of the members, which was accomplished by properly modifying the moment-rotation curve of the concentrated plasticity hinges, so that failure occurs when the moment reaches the value M_V that corresponds to the shear strength (i.e. for $M_V = V_R L_S$, where V_R is the shear strength and L_S is the shear length), if this happens before the failure in bending. According to the model proposed in the Greek Retrofitting Code, shear strength reduction due to cyclic response should also be taken into account, so the shear strength was assumed to be linearly reduced between $\mu_{\theta,pl} = 0$ and $\mu_{\theta,pl} = 5$. Schematically, the modification described above is shown in Fig. 5.

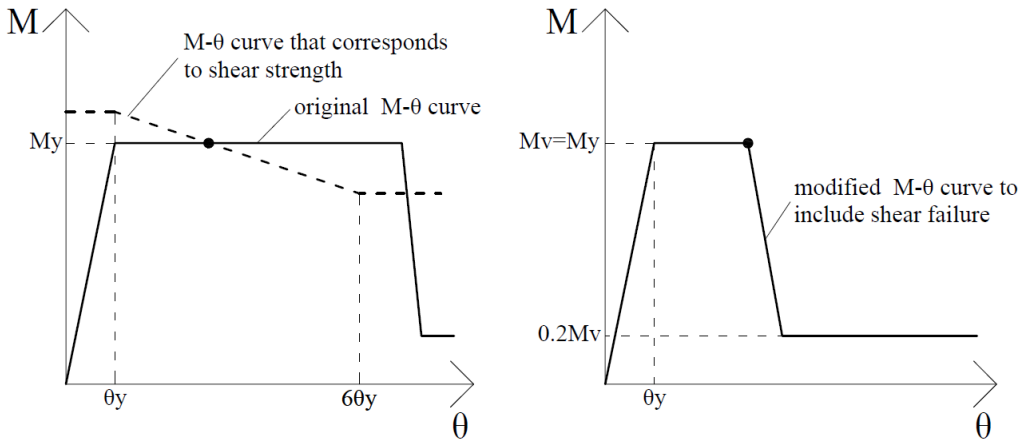

Figure 5. Modification of M-θ curves to include shear failure

Since the hinge and the stiffness characteristics of the members depend on the axial forces and the shear lengths of the members which change during the analysis, an iterative procedure was followed in order to consider representative values for the analysis, which were derived through pushover analyses at critical displacements in the four main directions. It was found that it was essential to use realistic values for the shear lengths to describe shear failure with the implicit method mentioned above.

The structural response analyses for static (pushover) and time-history excitations were performed using OpenSees and house programs for input data processing, model analysis and results processing.

ANALYSES RESULTS AND PROPOSED GROUND MOTION

The dynamic characteristics of the building under consideration are shown in Table 2. It is seen that the fundamental periods are 0.694 sec and 0.467 sec in the short and the long directions of the building, respectively, relatively small compared with the pulse period T_p = 1.6 sec considered in the ground motions. The aforementioned periods were calculated for elastic members with effective stiffness that corresponds to the yield moment and chord rotation, as suggested by EC8-3 and the Greek Retrofitting Code. The contribution of shear deformation and anchorage slip to the yield chord rotation, as mentioned earlier, was found to be significant compared to the chord rotation when only bending deformations were considered.

Table 2. Periods and effective modal mass ratio for excitations in the two main directions of the building under consideration

Period T (s)	Modal Mass (%)	
	Short direction	Long direction
0.694	68.7	0.0
0.555	5.1	0.5
0.467	0.1	82.2
0.202	14.0	0.0
0.181	0.5	0.1
0.159	0.0	9.7

It is noted that, in general, directivity effects alter significantly the response of the structures, even of small period, considerably less than the period of the directivity pulse, because, as the various members (beams, columns, infill walls) yield or fail, the period of the structure increases significantly. Directivity effects seem to produce more local failures and larger storey drifts, base shears and top displacements.

For the considered building, the influence of directivity in storey drifts is shown in Fig. 6, where the mean storey drifts in the two main directions are presented for the directivity pulse applied in the long or the short direction and two values of the standard deviation used in Eq. (3). It is evident that the addition of the directivity pulse in the ground motion increases the storey drifts in the corresponding direction, especially in the short direction of the building.

In Fig. 7, the results of the nonlinear analyses for different time-history scenarios are compared with the capacity (pushover) curve in the long direction of the building. Each point corresponds to the maximum base shear and the corresponding top displacement of a scenario, while the colours indicate the direction in which the directivity pulse was applied (green = no directivity pulse, blue = pulse applied in the long direction, red = pulse applied in the short direction). The number in the name of each point denotes the value of the fraction ε of the standard deviation. As can be seen, ground motion scenarios that include directivity phenomena in the examined direction (blue marks) seem to develop larger base shears and displacements.

It should be noted that, due to various uncertainties concerning the actual construction details of the building, the recorded damages could not be fully matched. Similar analyses for other buildings are needed to reach sound conclusions; in this sense, the results presented herein are considered preliminary.

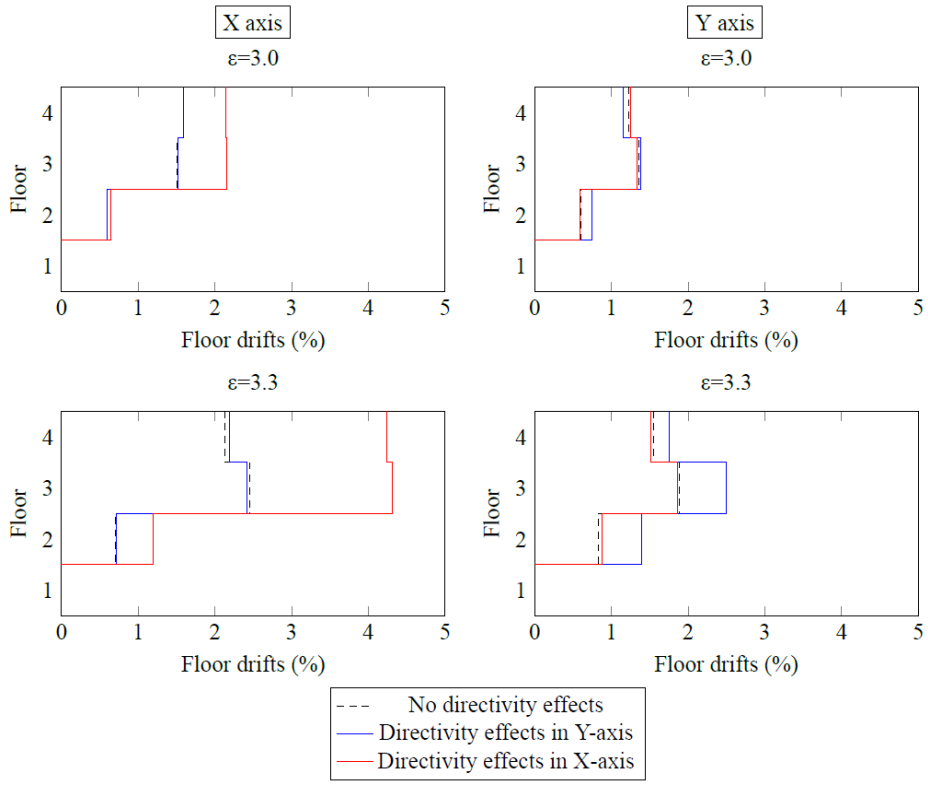

Figure 6. Mean storey drifts in two directions of the building for two cases of number of standard deviations considered and the directivity pulse applied to either of the main directions of the building under consideration

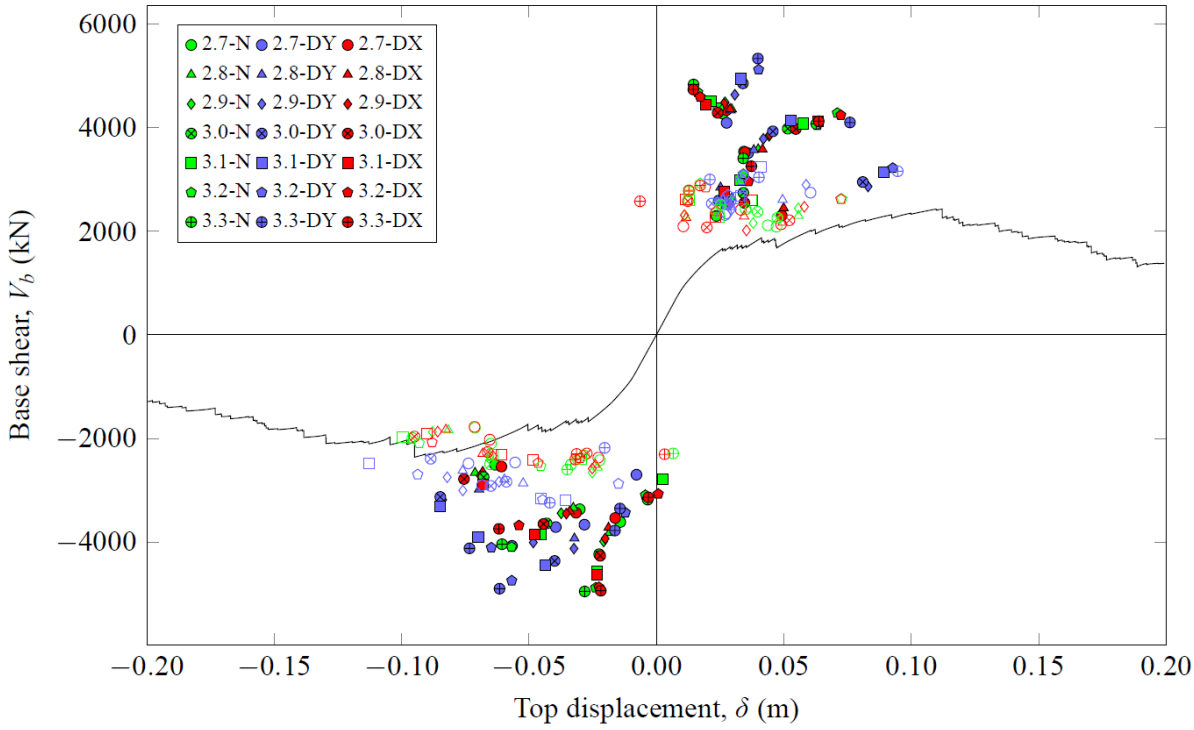

Figure 7. Comparison of the capacity (pushover) curve in the long direction of the building with the results of the nonlinear analyses for various ground motion scenarios

Table 3. Comparison of failures of ground-floor columns for some of the examined scenarios and for the directivity pulse applied in the long direction of the building

Number of standard deviations, **ε**	Based on	Number of failures in the short direction			Number of failures in the long direction		
		Common in reality and analysis	Only in reality	Only in the analysis	Common in reality and analysis	Only in reality	Only in the analysis
3.0	ATHA	0	5	1	4	8	0
3.0	SGMA	3	2	2	7	5	0
3.1	ATHA	1	4	1	7	5	0
3.1	SGMA	1	4	4	5	7	0
3.2	ATHA	2	3	2	6	6	0
3.2	DMK	4	1	4	6	6	0
3.2	SGMA	4	1	4	10	2	1
3.3	SGMA	4	1	5	11	1	2

Table 3 presents the comparison of the estimated damage (shear failure) to the columns of the ground floor with the observed damage for some of the scenarios considered with directivity effects in the direction of the long dimension of the building. Damage to other members remained at low levels, as observed in reality.

These results, and other similar ones not presented here, show that reasonable matching of the recorded damage, especially in what concerns shear failure of the columns of the ground floor (where most of the damage occurred), is achieved for peak ground acceleration (*PGA*) equal to about 0.69 g, corresponding to standard deviation fraction ε = 3.1 for the Boore & Atkinson spectra. This is especially true when directivity effects are considered in the long direction of the structure, in which most column failures were observed. The estimated value of the *PGA* shows that the seismic event was greater than what was widely thought.

In the short direction of the building, the observed failures were rather overestimated by the analyses for the same value of ε, especially when directivity phenomena were considered in that direction. It was found that a smaller value of standard deviation should be used, leading to less intense ground shaking. This is in accordance with observations of other researchers (Chioccarelli and Iervolino 2010) according to which the component of the ground motion that contains directivity pulses remains stronger than the other one, even after the removal of the pulses.

Based on the results of the nonlinear analyses and the comparison of the estimated damage with the observed one it can be concluded that directivity phenomena are pronounced in the long direction of the building, which is in accordance with the strong direction of the ground motion determined from the available records (Fig. 1). It is noted that this direction also coincides with the direction of toppling of rigid blocks and failures of simple structures in close areas that were observed after the earthquake, as reported bt the Technical Chamber of Greece (2001). Using data from those simple structures, the ground acceleration was assumed to have reached a value of about 0.50 g to 0.70 g, close to the one proposed here. However, the *PGA* for the specific area, estimated by theoretical analyses, was quite smaller, specifically 0.30 g to 0.50 g. For this reason, it was mentioned above that the estimated *PGA* of the ground motion with the present investigation is larger than what it was believed up to now.

The proposed mean spectra for the specific location can be seen in Fig. 8, with and without considering directivity effects. In the same figure, the elastic design spectra for the seismic zone of the site ($\gamma_I \cdot a_{gR}$ = 0.24 g) according to EC8 for soil categories A and B are shown for comparison. It can be seen that the estimated seismic excitation is generally larger than that assumed by the design code, especially in the short-period range. The proposed spectrum with directivity effects maintains large spectral acceleration values even in the medium period region. This means that significantly large ductility demands should have developed to typical structures with relatively small to medium fundamental periods.

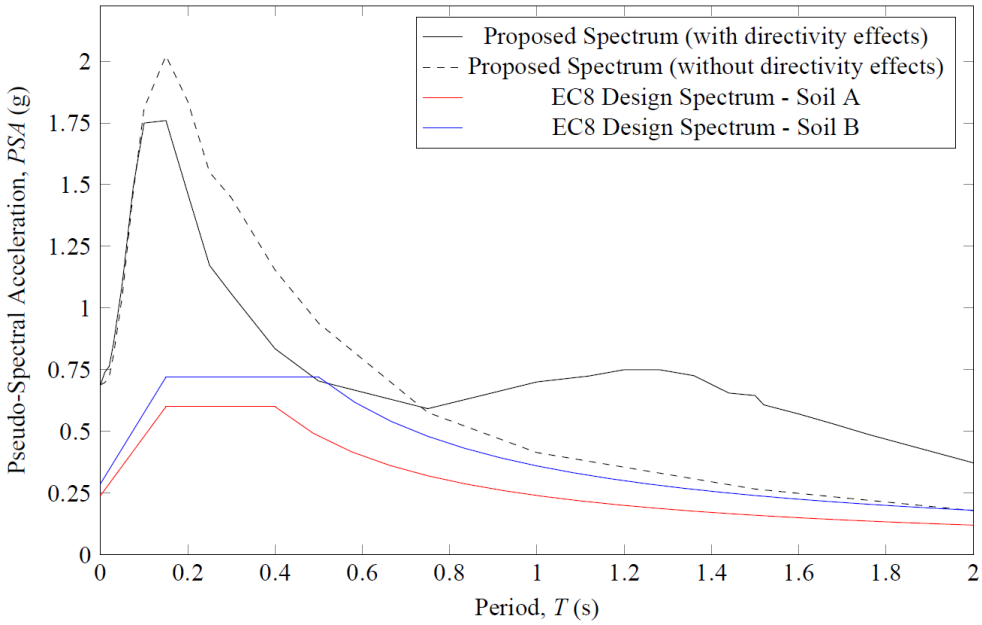

Figure 8. Proposed mean spectra for the site under examination and comparison with EC8 design spectra

CONCLUSIONS

Analysis of the recorded ground motions of the Athens 1999 earthquake showed that most of the recording sites were affected by forward directivity phenomena. The strong ground motion was oriented almost normal to the fault rupture direction, where directivity pulses were identified. Utilizing this information, the effect of the directivity phenomena on the damage to a typical reinforced concrete building in the most affected area was investigated. Based on the comparison of the computed damage, for various scenarios for the ground motion, with the observed one, conclusions were drawn concerning the peak ground acceleration and the response spectrum of the ground shaking in the examined area. The results need to be enhanced with similar analyses for other buildings in order to reach sound conclusions. The preliminary results presented herein show that directivity effects seem to have played a major role in developing structural damages, especially in the approximately normal to the rupture direction, while the estimated *PGA* of the ground motion (equal to 0.69 g) is larger than previous estimations.

ACKNOWLEDGEMENTS

The first author wants to thank the Greek State Scholarships Foundation for the financial support of his postgraduate studies at NTUA through “IKY Fellowships of excellence for postgraduate studies in Greece – Siemens program”.

REFERENCES

Abrahamson NA and Silva WJ (1997) “Empirical response spectral attenuation relationships for shallow crustal earthquakes”, *Seismological Research Letters*, 68(1): 94-127

Bertero VV, Mahin SA and Herrera RA (1978), “Aseismic design implications of near-fault San Fernando earthquake records” *Earthquake engineering & structural dynamics*, 6(1): 31-42

Boore DM and Atkinson GM (2008) “Ground-motion prediction equations for the average horizontal component of PGA, PGV, and 5%-damped PSA at spectral periods between 0.01s and 10.0 s”, *Earthquake Spectra*, 24(1): 99–138

Chioccarelli E and Iervolino I (2010) “Near-source seismic demand and pulse-like records: A discussion for L'Aquila earthquake”, *Earthquake Engineering and Structural Dynamics*, 39(9): 1039-1062

Earthquake Planning and Protection Organization (2012) Greek Retrofitting code (KAN.EPE.), Athens (in Greek)

Elenas A (2003) "Athens earthquake of 7 September 1999: Intensity measures and observed damages", *ISET Journal of Earthquake Technology*, 40(1): 77–97

European Committee for Standardization (2005) European Standard EN 1998-3:2005 Eurocode 8. Design of Structures for Earthquake Resistance - Part 3: Assessment and Retrofitting of Buildings, Brussels

Ibarra LF and Krawinkler H (2005) Global collapse of frame structures under seismic excitations, Report #152, Stanford (CA): John A. Blume Earthquake Engineering Center

Iervolino I and Cornell CA (2008) "Probability of occurrence of velocity pulses in near-source ground motions", *Bulletin of the Seismological Society of America*, 98(5): 2262-2277

OpenSees v.2.4.3, Pacific Earthquake Engineering Research Center, University of California, Berkeley, CA, http://opensees.berkeley.edu/

Psycharis I, Papastamatiou D, Taflambas I, Carydis P (1999) The Athens Earthquake of September 7, 1999, Reconnaissance report, EERI Newsletter

Rowshandel B (2006) "Incorporating source rupture characteristics into ground-motion hazard analysis models", *Seismological Research Letters*, 77(6): 708-722

Seismosoft "SeismoMatch", v2.1, http://www.seismosoft.com/en/SeismoMatch.aspx

Shahi SK and Baker JW (2011) "An empirically calibrated framework for including the effects of near-fault directivity in probabilistic seismic hazard analysis", *Bulletin of the Seismological Society of America*, 101(2): 742–755

Somerville PG (2003) "Magnitude scaling of the near fault rupture directivity pulse" *Physics of the earth and planetary interiors*, 137(1): 201-212

Somerville PG (1998) "Development of an improved representation of near fault ground motions" *SMIP98 Seminar on Utilization of Strong-Motion Data* (Vol. 15)

Somerville PG, Smith NF, Graves RW and Abrahamson NA (1997) "Modification of empirical strong ground motion attenuation relations to include the amplitude and duration effects of rupture directivity" *Seismological Research Letters*, 68(1): 199-222

Technical Chamber of Greece (2001) Study of the Athens 7-9-99 earthquake, Computational estimation of accelerations in the most-damaged areas (in Greek)